ACS APPLIED MATERIALS & INTERFACES

Research Article

www.acsami.org

Synthesis of One-Dimensional CdS@TiO_2 Core–Shell Nanocomposites Photocatalyst for Selective Redox: The Dual Role of TiO_2 Shell

Siqi Liu,[†,‡] Nan Zhang,[†,‡] Zi-Rong Tang,[‡] and Yi-Jun Xu*[,†,‡]

[†]State Key Laboratory Breeding Base of Photocatalysis, College of Chemistry and Chemical Engineering, Fuzhou University, Fuzhou, 350002, People's Republic of China

[‡]College of Chemistry and Chemical Engineering, New Campus, Fuzhou University, Fuzhou, 350108, People's Republic of China

Supporting Information

ABSTRACT: One-dimensional (1D) CdS@TiO_2 core–shell nanocomposites (CSNs) have been successfully synthesized via a two-step solvothermal method. The structure and properties of 1D CdS@TiO_2 core–shell nanocomposites (CdS@TiO_2 CSNs) have been characterized by a series of techniques, including X-ray diffraction (XRD), ultraviolet–visible-light (UV-vis) diffuse reflectance spectra (DRS), field-emission scanning electron microscopy (FESEM), photoluminescence spectra (PL), and electron spin resonance (ESR) spectroscopy. The results demonstrate that 1D core–shell structure is formed by coating TiO_2 onto the substrate of CdS nanowires (NWs). The visible-light-driven photocatalytic activities of the as-prepared 1D CdS@TiO_2 CSNs are evaluated by selective oxidation of alcohols to aldehydes under mild conditions. Compared to bare CdS NWs, an obvious enhancement of both conversion and yield is achieved over 1D CdS@TiO_2 CSNs, which is ascribed to the prolonged lifetime of photogenerated charge carriers over 1D CdS@TiO_2 CSNs under visible-light irradiation. Furthermore, it is disclosed that the photogenerated holes from CdS core can be stuck by the TiO_2 shell, as evidenced by controlled radical scavenger experiments and efficiently selective reduction of heavy-metal ions, Cr(VI), over 1D CdS@TiO_2 CSNs, which consequently leads to the fact that the reaction mechanism of photocatalytic oxidation of alcohols over 1D CdS@TiO_2 CSNs is apparently different from that over 1D CdS NWs under visible-light irradiation. It is hoped that our work could not only offer useful information on the fabrication of various specific 1D core–shell nanostructures, but also open a new doorway of such 1D core–shell semiconductors as visible-light photocatalysts in the promising field of selective transformations.

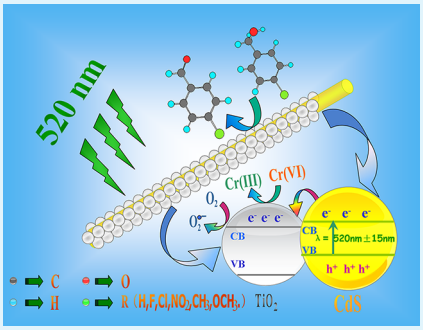

KEYWORDS: *one-dimensional, core–shell nanocomposite, visible-light photocatalyst, selective oxidation, mild conditions*

1. INTRODUCTION

Core–shell nanocomposites (CSNs), including multiphase semiconductors, metal–semiconductors, and metal–metal nanocomposites, have been the subject of extensive research, because of their tunable surface properties, enhanced optical, electronic, catalytic properties, and their potential applications in many areas such as microelectronics, optoelectronics, optical devices, and catalysis in the past decades.[1−18] Compared to the single-component counterparts, CSNs exhibit improved physical and chemical properties, thus providing a new way to tailor the properties of the nanomaterials.[19] For example, semiconductor–semiconductor CSNs with matchable band structures and metal–semiconductor CSNs are of particular interest to photocatalytic applications.[5−7,19−23] As a member of core–shell structural nanocomposites family, one-dimensional (1D) core–shell nanocomposites that are utilized as photocatalysts have received a great deal of research interest, because of their unique structural and electronic properties in recent years.[24−26] In contrast to nanoparticles or bulk materials, 1D structural CSNs have unique advantages as potential photocatalysts.[27−30] First, the 1D geometry leads to a fast and long-distance electron transport. Second, the light absorption and scattering can be obviously enhanced because of the high length-to-diameter ratio of the 1D structure. Third, 1D structures are expected to have larger specific surface area and pore volume, compared to the particle counterparts. Thus, the 1D CSNs combined the core–shell structure with 1D structure are expected to be worthy of intriguing exploration. Furthermore, the photocatalytic applications for the 1D CSNs often involve "non-selective" degradation of pollutants or water splitting.[25,26,31−33] However, the application of CSNs in the field of photocatalytic selective transformation still remains very limited.[19]

In recent years, a great deal of attention has been devoted to utilization of photocatalytic processes for oxofunctionalization of hydrocarbons, namely, selective organic transformations under ambient conditions because of its environmental

Received: September 21, 2012
Accepted: November 6, 2012
Published: November 6, 2012

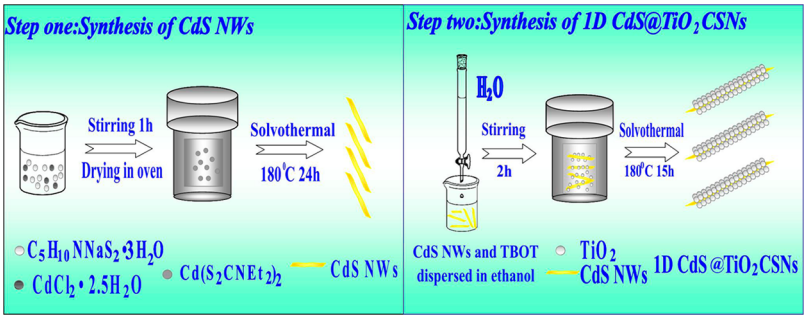

Figure 1. Schematic flowchart for two-step synthesis of 1D CdS@TiO_2 CSNs.

friendliness and promising potential as a green technique.[20,34−37] Among the various organic reactions, selective oxidation of alcohols to carbonyls is a fundamental but significant transformation for the synthesis of fine chemicals, because carbonyl compounds such as ketone and aldehyde derivatives are widely utilized in the fragrance, confectionary, and pharmaceutical industries.[7,38,39] Thus, increasing efforts have been paid to the photocatalytic selective oxidation of alcohols.[6,7,34−44] However, most of the reports on photocatalysis used for selective oxidation of alcohols are focused on TiO_2 or TiO_2-based materials.[37−50] Therefore, it is of fundamental interest to exploit new type visible-light-driven photocatalysts, e.g., the aforementioned semiconductor 1D CSNs, for photocatalytic selective transformations under ambient conditions.

As two of the mostly studied semiconductor photocatalysts in practical applications, CdS and TiO_2 have attracted great attention, and to make better use of them, these two semiconductors are often coupled each other, because of their matched band structures. Hitherto, many attempts have been explored to fabricate and utilize the CdS/TiO_2 1D CSNs as photocatalysts.[25,31,51,52] For instance, Misra and co-workers synthesized 1D CdS@TiO_2 CSNs by filling 1D TiO_2 nanotubes with CdS nanoparticles.[25] The 1D CdS@TiO_2 CSNs exhibited obvious enhanced activity for H_2 generation from water, compared to TiO_2 nanotubes.[25] Cho et al. reported self-organized TiO_2 nanotube arrays decorated by CdS quantum dots uniformly via a sonication-assisted sequential chemical bath deposition (S-CBD) approach.[31] The obtained products possessed higher activity than TiO_2 nanotube arrays for photocatalytic degradation of Methyl Orange (MO) under visible-light illumination.[31] However, most reports often involve 1D TiO_2 as building blocks, whereas the use of 1D CdS as substrates is scarce.[25,31,53−55] In addition, the 1D structure building blocks are often synthesized by a chemical vapor deposition (CVD) method,[56] an electrochemical method[25,57] and a template method,[58] which frequently involve high temperature, multiple steps, and long periods of time. Thus, it is desirable to exploit a facile and template-free way to synthesize 1D CSNs. In particular, the use of 1D CSNs for photocatalytic selective transformation has been unavailable so far in heterogeneous photocatalysis.

Herein, we report a facile, template-free synthesis of 1D CdS@TiO_2 core−shell nanocomposites (CdS@TiO_2 CSNs) via a two-step solvothermal method. Taking photocatalytic selective oxidation of alcohols as probing reactions, the photoactivity has been investigated under visible-light irradiation. The results show that the 1D CdS@TiO_2 CSNs exhibit enhanced photocatalytic performance, compared to that of bare CdS nanowires (NWs), toward selective oxidation of alcohols to corresponding aldehydes under ambient conditions (i.e., room temperature and atmospheric pressure). The TiO_2 shell in 1D CdS@TiO_2 CSNs not only allows the photogenerated electrons from CdS core to transfer to its conduction band, but also suppresses the tunneling of the photogenerated holes from the CdS core to the surface of the TiO_2 shell. Therefore, the photogenerated holes do not play a distinct role in selective oxidation of alcohols over 1D CdS@TiO_2 CSNs under visible-light irradiation, which is evidenced by the controlled radical scavengers experiments and efficiently selective reduction of heavy-metal ions, Cr(VI), over 1D CdS@TiO_2 CSNs. To the best of our knowledge, this work represents the first example to use the 1D core−shell semiconductor composite photocatalyst for selective oxidation and reduction reaction. It is expected that our work could open a new stepping stone for the utilization of such 1D core−shell semiconductor composites as visible-light photocatalysts for selective organic transformations.

2. EXPERIMENTAL SECTION

2.1. Materials. Sodium diethyldithiocarbamate trihydrate ($C_5H_{10}NNaS_2·3H_2O$), tetrabutyl titanate (TBOT, $C_{16}H_{36}O_4Ti$), cadmium chloride ($CdCl_2·2.5H_2O$), ethylenediamine ($C_2H_8N_2$), and ethanol (C_2H_6O) were obtained from Sinopharm Chemical Reagent Co., Ltd. (Shanghai, China). All materials were used as received without further purification. Deionized water that was used in the synthesis was obtained from local sources.

2.2. Catalyst Preparation. The 1D CdS@TiO_2 core−shell nanocomposites (CSNs) have been fabricated by a facile and template-free two-step solvothermal method, as illustrated in Figure 1.

(a). The First Step is the Synthesis of CdS Nanowires. Uniform CdS NWs were grown through a modified method.[59] In a typical process, 1.124 g of cadmium diethyldithiocarbamate ($Cd(S_2CNEt_2)_2$), prepared by precipitation from a stoichiometric mixture of sodium diethyldithiocarbamate trihydrate and cadmium chloride in deionized water, was added to a Teflon-lined stainless steel autoclave with a capacity of 50 mL. Then, the autoclave was filled with 40 mL of ethylenediamine to ∼80% of the total volume. The autoclave was maintained at 180 °C for 24 h and then allowed to cool to room temperature. A yellowish precipitate was collected and washed with absolute ethanol and deionized water to remove residue of organic solvents. The final products were dried in an oven at 60 °C for 12 h.

(b). The Second Step is the Synthesis of 1D CdS@TiO_2 CSNs. The composites were synthesized by a wet-chemistry method and tetrabutyl titanate (TBOT) was used as the titania source. First, a certain amount of the CdS NWs and TBOT were sonicated thoroughly in 50 mL of absolute ethanol for 15 min. Then, 30 mL of deionized water was added dropwise, with magnetic stirring. After stirring for 2 h, the yellow solution was transferred into a 100-mL stainless steel autoclave with a Teflon liner and kept at 180 °C for 15 h. The yellow precipitates thus obtained were collected, washed thoroughly with deionized water, and then dried in an oven at 60 °C. The molar ratio of CdS to TiO_2 was 1:3.

2.3. Catalyst Characterization. The crystal phase properties of the samples were analyzed with a Bruker D8 Avance X-ray diffractometer (XRD) using Ni-filtered Cu Kα radiation at 40 kV and 40 mA in the 2θ range of 20°−80°, with a scan rate of 0.02° per second. The optical properties of the samples were characterized by a Cary 500 UV-vis ultraviolet/visible diffuse reflectance spectrophotometer (DRS), during which $BaSO_4$ was employed as the internal reflectance standard. Field-emission scanning electron microscopy (FESEM) was used to determine the morphology of the samples on a FEI Nova NANOSEM 230 spectrophotometer. The photoluminescence (PL) spectra for solid samples were investigated on a Cary Eclipse Fluorescence spectrophotometer. The electron spin resonance (ESR) signal of the radicals spin-trapped by 5,5-dimethyl-l-pyrroline-*N*-oxide (DMPO, supplied from Sigma Co., Ltd.) was recorded on a Bruker EPR A300 spectrometer. In detail, the sample (5 mg) was dispersed in 0.5 mL of purified benzotrifluoride (BTF), into which 25 μL of DMPO/benzyl alcohol solution (1:10, v/v) was added. The mixture was oscillated to obtain a well-blended suspension. The irradiation source (λ = 520 ± 15 nm) was a 300 W Xe arc lamp system, which was the very light source for our photocatalytic selective oxidation of alcohols. The settings for the ESR spectrometer were as follows: center field = 3512 G, microwave frequency = 9.86 GHz, and power = 2.00 mW.

2.4. Catalyst Activity. The photocatalytic selective oxidation of various alcohols was performed as follows. A mixture of alcohol (0.1 mmol) and 8 mg of catalyst was dissolved in the solvent of benzotrifluoride (BTF, supplied from Alfa Aesar with a purity of >99%) (1.5 mL), which was saturated with pure molecular oxygen. The choice of solvent BTF is because of its inertness to oxidation and high solubility for molecular oxygen.[6,30,37,39] The above mixture was transferred into a 10-mL Pyrex glass bottle filled with molecular oxygen at a pressure of 0.1 MPa and stirred for half an hour to make the catalyst blend evenly in the solution. The suspensions were irradiated by a 300 W Xe arc lamp (PLS-SXE 300, Beijing Perfectlight Co., Ltd.) with a UV-CUT filter and a band-pass filter to make the wavelength of incident light at λ = 520 ± 15 nm. After the reaction, the mixture was centrifuged at 12 000 rmp for 20 min to completely remove the catalyst particles. The remaining solution was analyzed with an Agilent gas chromatograph (Model GC-7820, with a capillary FFAP analysis column). Controlled photoactivity experiments using different radical scavengers (ammonium oxalate as a scavenger for photogenerated holes,[5,60,61] $AgNO_3$ as a scavenger for electrons,[60,62,63] *tert*-butyl alcohol as a scavenger for hydroxyl radicals,[5,64] and benzoquinone as a scavenger for superoxide radical species[60,65]) were performed, similar to the above photocatalytic oxidation of alcohols, except that the radical scavengers (0.1 mmol) were added to the reaction system. The conversion of alcohol, the yield of aldehyde, and the selectivity for aldehyde were defined as follows:

$$\text{conversion}\,(\%) = \left(\frac{C_0 - C_{\text{alcohol}}}{C_0}\right) \times 100$$

$$\text{yield}\,(\%) = \left(\frac{C_{\text{aldehyde}}}{C_0}\right) \times 100$$

$$\text{selectivity}\,(\%) = \left(\frac{C_{\text{aldehyde}}}{C_0 - C_{\text{alcohol}}}\right) \times 100$$

where C_0 is the initial concentration of alcohol; C_{alcohol} and C_{aldehyde} are the concentrations of the substrate alcohol and the corresponding aldehyde, respectively, at a certain time after the photocatalytic reaction.

3. RESULTS AND DISCUSSION

The crystallographic structure of the as-prepared CdS NWs and 1D CdS@TiO_2 core−shell nanocomposites (CdS@TiO_2 CSNs) are examined by powder X-ray diffraction (XRD). The XRD data are shown in Figure 2. The as-prepared CdS NWs and 1D CdS@TiO_2 CSNs exhibit similar diffraction peaks, in terms of CdS framework, in which the peaks at 2θ values of 24.8°, 26.5°, 28.2°, 36.6°, 43.7°, 47.9°, 50.9°, 51.8°, 52.8°, 66.8°, 69.2°, 70.9°, 72.3°, and 75.4° can be attributed to the (100), (002), (101), (102), (110), (103), (200), (112), (201), (203), (210), (211), (114), and (105) crystal planes of greenokite structure CdS (JCPDS No. 41-1049), respectively. The weaker diffraction peaks of CdS in the 1D CdS@TiO_2 CSNs than those of CdS NWs may result from the possible structure that TiO_2 is densely coated on the surface of the CdS NWs, which is verified by the following scanning electron microscopy (SEM) analysis. In addition, a typical diffraction peak of TiO_2, located at 2θ = 25.3°, is observed in 1D CdS@TiO_2 CSNs, which is attributed to the (101) crystal planes of anatase-phase TiO_2 (JCPDS No. 21-1272).

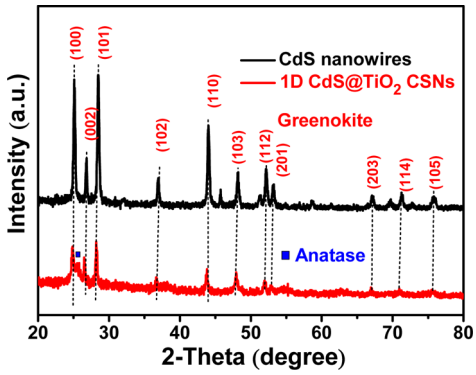

Figure 2. XRD patterns of the as-prepared samples of CdS NWs and 1D CdS@TiO_2 CSNs.

Figure 3 shows the typical SEM images of 1D CdS NWs and 1D CdS@TiO_2 CSNs resulting from the coating of TiO_2 onto 1D CdS NWs. As seen in Figures 3A and 3B, the as-prepared CdS NWs exhibit the 1D morphology with an average length of ca. 2−3 μm and an average diameter of ca. 50−100 nm. The dimensions are highly uniform among individual NWs, which is consistent with the previous report.[59] After the deposition of TiO_2 onto the CdS NWs, it can be seen from Figures 3C and 3D that TiO_2 particles are densely coated onto the wall of CdS NWs, thereby forming the 1D CdS@TiO_2 CSNs. It is clear that, during the formation process of 1D CdS@TiO_2 CSNs, the uniformly dispersed 1D CdS NWs in solution serve as heterogeneous seeds around which TiO_2 shell grows, i.e., a well-known heterogeneous seeded growth process.[66−68] The SEM results suggest that the 1D CdS@TiO_2 CSNs have been achieved via a carefully controlled two-step solvothermal process.

The UV-vis diffuse reflectance spectra (DRS) are used to determine the optical properties of the samples. Figure 4 shows that the dense coating of TiO_2 onto 1D CdS NWs has a significant effect on the optical property of light absorption for the as-prepared 1D CdS@TiO_2 CSNs in the ultraviolet (UV) region. It is clear that the 1D CdS@TiO_2 CSNs exhibit significantly enhanced light absorption capacity in the UV region, compared to 1D CdS NWs. With the addition of TiO_2, there is enhanced absorption intensity for UV light. This is understandable because TiO_2 by itself has strong UV light absorption. In contrast, because TiO_2 does not have visible-light absorption, the coating of TiO_2 onto yellow 1D CdS NWs will decrease the visible-light absorption capacity of 1D CdS@TiO_2 CSNs, compared to the original 1D CdS NWs. In addition, the DRS spectra indicate that both 1D CdS@TiO_2

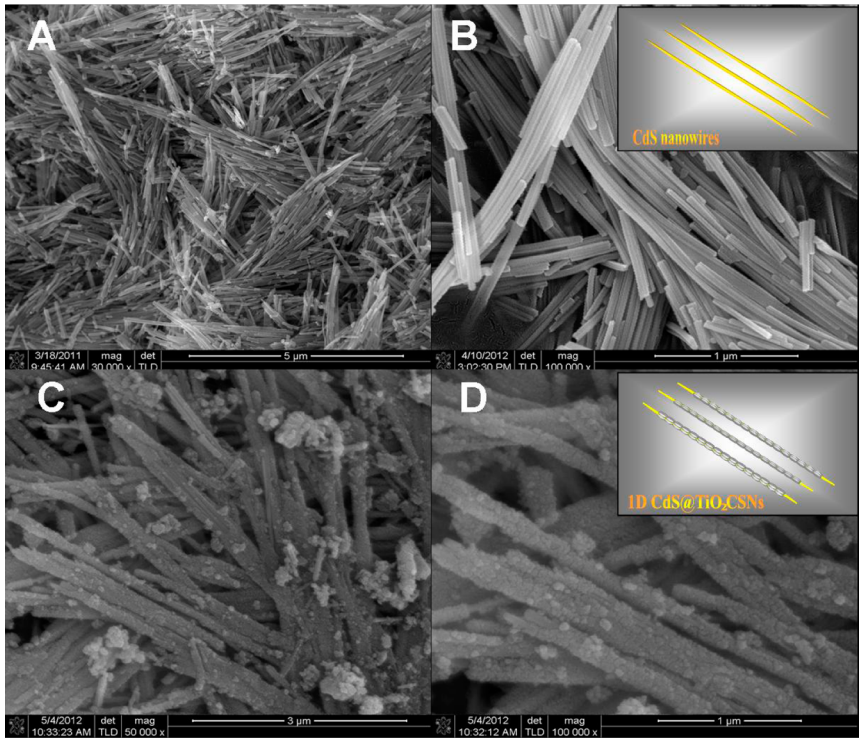

Figure 3. Typical SEM images of the as-prepared samples of (A, B) CdS NWs and (C, D) 1D CdS@TiO_2 CSNs at different magnifications; the insets of B and D are the corresponding schematic models.

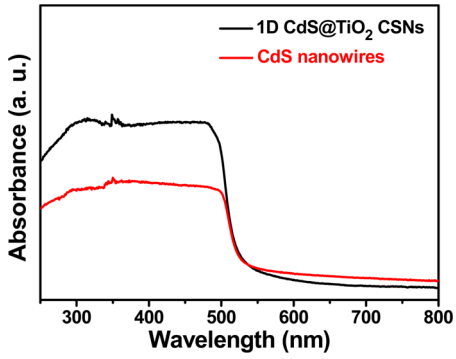

Figure 4. UV-vis diffuse reflectance spectra (DRS) of the samples of CdS NWs and 1D CdS@TiO_2 CSNs.

CSNs and CdS NWs are able to be photoexcited by visible-light irradiation, by which chemical redox reactions could be triggered.

The photocatalytic activity of 1D CdS@TiO_2 CSNs has been evaluated by the aerobic selective oxidation of alcohols to corresponding aldehydes under visible-light irradiation under ambient conditions, i.e., room temperature and atmospheric pressure. As shown in Table 1, it can be observed that both the CdS NWs and 1D CdS@TiO_2 CSNs are visible-light-active for the photocatalytic selective oxidation of alcohols into corresponding aldehydes. The 1D CdS@TiO_2 CSNs exhibit higher photoactivity than CdS NWs in all selected reactions of oxidation of various alcohols. For example, under visible-light irradiation for 8 h, the conversion for benzyl alcohol (BA) and yield for benzaldehyde (BAD) are ~34% and ~33% over the 1D CdS@TiO_2 CSNs, respectively, which is much higher than the values obtained over CdS NWs (13% conversion and 12% yield). The similar photoactivity enhancement trend can also be found in selective oxidation of other alcohols, such as *p*-fluoro benzyl alcohol, *p*-nitro benzyl alcohol, *p*-chloro benzyl alcohol, *p*-methyl benzyl alcohol, and *p*-methoxyl benzyl alcohol. Thus, it can be concluded that coating TiO_2 onto the 1D CdS NWs can significantly enhance the photocatalytic activity of semiconductor CdS NWs toward selective oxidation of alcohol

Table 1. Photocatalytic Selective Oxidation of a Series of Alcohols into Corresponding Aldehydes over CdS NWs and 1D CdS@TiO_2 CSNs under Visible Light ($\lambda = 520 \pm 15$ nm) Irradiation for 8 h

			Conversion (%)		Yield (%)		Selectivity (%)	
Entry	Substrate	Product	CdS	CdS@TiO_2	CdS	CdS@TiO_2	CdS	CdS@TiO_2
1	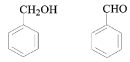		13	34	12	33	97	97
2	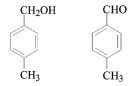		7	41	4	30	60	74
3	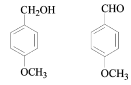		21	39	8	25	36	65
4	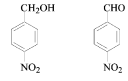		7	30	5	21	73	70
5	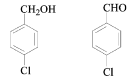		4	38	3	33	88	87
6	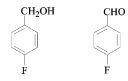		6	37	5	36	97	96

dx.doi.org/10.1021/am302074p | *ACS Appl. Mater. Interfaces* 2012, 4, 6378−6385

under visible-light illumination. In addition, it should be noted that no conversion of alcohols is observed in the blank experiments performed in the absence of catalyst and/or visible light, which confirms that the reaction is really driven by a photocatalytic process.

The photoactivity testing on used 1D CdS@TiO_2 CSNs shows this photocatalyst is stable and reusable in the reaction medium of BTF solvent. As shown in Figure S1 in the Supporting Information, after recycling photoactivity test for the selective oxidation of benzyl alcohol (BA) 4 times, the yield of benzaldehyde (BAD) over used 1D CdS@TiO_2 CSNs is similar to that over fresh 1D CdS@TiO_2 CSNs. Therefore, the as-prepared 1D CdS@TiO_2 CSNs semiconductor is a stable visible-light-driven photocatalyst for the selective oxidation of BA in the reaction medium of BTF solvent under ambient conditions.

To further understand the higher photocatalytic activity of 1D CdS@TiO_2 CSNs for selective oxidation of alcohols than the original 1D CdS NWs, we probe into a possible reason on the basis of theoretical and experimental analysis. TiO_2 has the band structures with suitable position for CdS in the CdS–TiO_2 integrated system; the conduction band (CB) of TiO_2 is less negative than the CB of CdS. Therefore, the photogenerated electrons from CdS could transfer to the CB of TiO_2. Thus, the separation of photoinduced electron–hole pairs is improved and the lifetime of the carriers is prolonged, indicating that the recombination of photogenerated electron–hole pairs is hampered in the 1D CdS@TiO_2 CSNs, compared to the 1D CdS NWs. This prolonged lifetime of the photogenerated charge carriers can be confirmed by the photoluminescence (PL) spectra. As displayed in Figure 5,

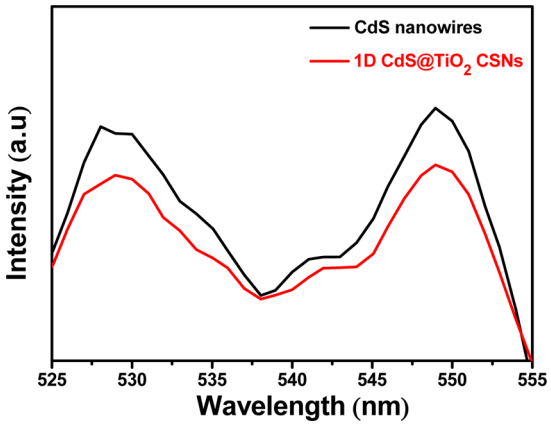

Figure 5. Photoluminescence (PL) spectra of CdS NWs and 1D CdS@TiO_2 CSNs.

under an excitation wavelength of 403 nm, the PL intensity obtained over 1D CdS@TiO_2 CSNs is much weaker than that of CdS NWs, thus suggesting the longer lifetime of photogenerated charge carriers from 1D CdS@TiO_2 CSNs. The two distinct green emission bands at ~528 and 550 nm can be observed, which is consistent with the previous reports.[69−71] The former one can be assigned to near-band-edge emission, and the latter is associated with structural defects that may arise from the excess of sulfur or core defects on the nanowire surfaces.[69−71] The charge carriers with prolonged lifetime photoinduced from 1D CdS@TiO_2 CSNs are beneficial for the enhanced photocatalytic activity over the original 1D CdS NWs.

For an in-depth understanding of the role of photogenerated radical species on the selective oxidation of alcohols over the 1D CdS@TiO_2 CSNs photocatalyst, we have further performed a series of controlled experiments. A controlled experiment, carried out in the presence of nitrogen, shows that only trace conversion of benzyl alcohol is detected, demonstrating that oxygen as a primary oxidant is essential during the photocatalytic process. Controlled experiments using different radical scavengers help us to further understand the role of photogenerated radical species and the underlying reaction mechanism for the selective oxidation of alcohols over the 1D CdS NWs and 1D CdS@TiO_2 CSNs under visible-light irradiation.

Figure 6 shows the results of adding different radical scavengers over the 1D CdS NWs photocatalyst reaction

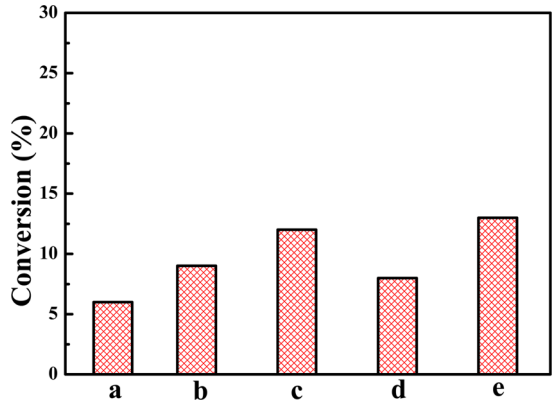

Figure 6. Controlled experiments using different radical scavengers for the photocatalytic selective oxidation of benzyl alcohol (BA) over CdS NWs in the BTF solvent; (a) reaction with $AgNO_3$ as a scavenger for photogenerated electrons, (b) reaction with benzoquinone (BQ) as a scavenger for superoxide radicals, (c) reaction with *tert*-butyl alcohol (TBA) as scavenger for hydroxyl radicals, (d) reaction with ammonium oxalate (AO) as a scavenger for photogenerated holes, and (e) the reaction in the absence of radical scavengers under visible-light irradiation for 8 h.

system under visible-light irradiation. When the radical scavenger, ammonium oxalate (AO), for holes[5,60,61] is added into the reaction system, the conversion of benzyl alcohol is significantly inhibited (entry d in Figure 6). A similar and obvious inhibition phenomenon for the photocatalytic reaction is also observed when the $AgNO_3$ scavenger for electrons[60,62,63] and the benzoquinone (BQ) scavenger for superoxide radicals ($O_2^{\bullet -}$)[60,65] are added into the reaction system (see entries a and b in Figure 6, respectively). These results clearly suggest that the photocatalytic oxidation of benzyl alcohol over the 1D CdS NWs is primarily driven by photogenerated holes, electrons, and $O_2^{\bullet -}$. Notably, the existence of $O_2^{\bullet -}$ in the reaction system has been verified by the electron spin resonance (ESR) spectra (see Figure S2 in the Supporting Information). However, strong and nonselective hydroxyl radicals are not detected by the ESR analysis, which is consistent with previous works regarding the photocatalytic selective oxidation of alcohols in a solvent of benzotrifluoride (BTF).[6,39,72] Indeed, the addition of the scavenger, *tert*-butyl alcohol (TBA), for hydroxyl radicals,[5,64] into the reaction system has a negligible effect on the conversion of benzyl alcohol, as reflected by entry c in Figure 6, which is consistent with the absence of hydroxyl radicals in the BTF solvent.[37,39,72]

Interestingly, a different phenomenon is achieved from the controlled experiments over 1D CdS@TiO_2 CSNs photocatalysts. As shown in entries a and b in Figure 7, when the

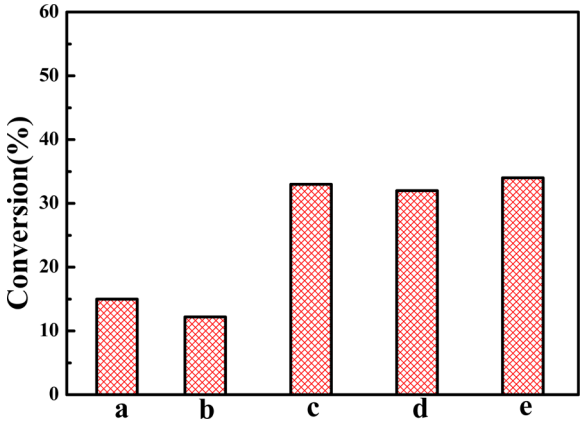

Figure 7. Controlled experiments using different radical scavengers for the photocatalytic selective oxidation of benzyl alcohol (BA) over 1D CdS@TiO_2 CSNs in the BTF solvent; (a) reaction with $AgNO_3$ as a scavenger for photogenerated electrons, (b) reaction with benzoquinone (BQ) as a scavenger for superoxide radicals, (c) reaction with *tert*-butyl alcohol (TBA) as a scavenger for hydroxyl radicals, (d) reaction with ammonium oxalate (AO) as a scavenger for photogenerated holes, and (e) reaction in the absence of radical scavengers under visible-light irradiation for 8 h.

radical scavenger of $AgNO_3$ for electrons[60,62,63] and BQ for $O_2^{\bullet -}$ are added,[60,65] respectively, the photocatalytic reaction is significantly inhibited. However, there is almost no change for the conversion of benzyl alcohol when using AO as the radical scavenger for holes (entry d in Figure 7).[5,60,61] This phenomenon can be due to the fact that the thick TiO_2 shell suppresses the tunneling of the holes from the CdS NWs to the surface atoms of the shell, resulting in the blockage of holes.[24] It should be noted that, under visible light (λ = 520 ± 15 nm) irradiation, only the semiconductor CdS NWs in the core is able to be "band-gap-photoexcited" to produce electron−hole pairs while the semiconductor TiO_2 in the shell cannot be photoexcited. Thus, although the TiO_2 shell improves the lifetime of photogenerated charge carriers of 1D CdS@TiO_2 CSNs resulting from the transfer of photoexcited electrons from CdS core, it can also block the photoexcited holes from CdS core moving to the surface of TiO_2 shell. As a result, the contribution of photogenerated holes to photocatalytic oxidation of alcohols over 1D CdS@TiO_2 CSNs is significantly weakened, compared to 1D CdS NWs. The reaction over 1D CdS@TiO_2 CSNs is primarily driven by photogenerated electrons and $O_2^{\bullet -}$. In addition, similar to the observation over 1D CdS NWs photocatalyst, the addition of *tert*-butyl alcohol (TBA)[5,64] does not almost affect the photocatalytic conversion over 1D CdS@TiO_2 CSNs, as reflected by entry c in Figure 7, which is in agreement with the absence of hydroxyl radicals in the BTF solvent.[37,39,72]

As mentioned above, since the holes photoexcited from CdS core can be stuck by the TiO_2 shell for 1D CdS@TiO_2 CSNs while electrons are able to move to the surface of TiO_2 shell, the 1D CdS@TiO_2 CSNs should be also efficient for photocatalytic selective reduction reaction. This inference is faithfully evidenced by photocatalytic reduction of heavy-metal ions, Cr(VI), as displayed in Figure S3 in the Supporting Information. It is observed that 1D CdS@TiO_2 CSNs exhibit an excellent photocatalytic performance for selective reduction of Cr(VI) to Cr(III) under visible-light irradiation; within 30 min, the conversion reaches 100%, which is significantly much higher than 1D CdS NWs. This is understandable because (i) the photogenerated electrons from 1D CdS@TiO_2 CSNs are more easily accessible than that for 1D CdS NWs under visible-light irradiation, which results in more-efficient reduction of Cr(VI) via capturing electrons; (ii) the lifetime of charge carriers over 1D CdS@TiO_2 CSNs is enhanced, compared to 1D CdS NWs under visible-light irradiation.

Based on the above discussion, a tentative reaction mechanism has been proposed, as illustrated in Figure 8.

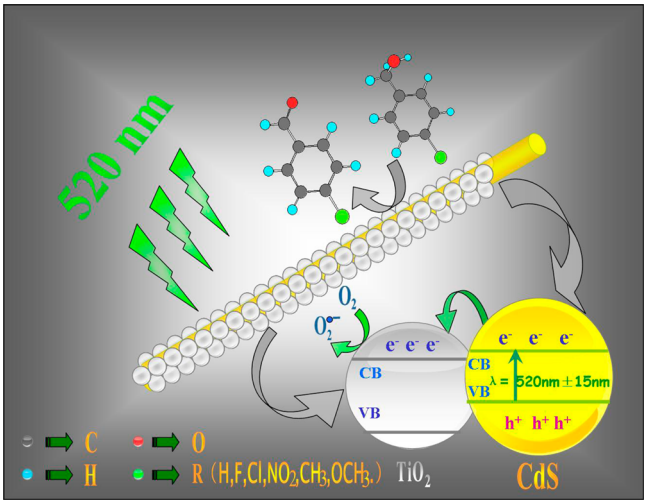

Figure 8. Illustration of the proposed reaction mechanism for selective oxidation of alcohols to corresponding aldehydes over the 1D CdS@TiO_2 CSNs under visible-light irradiation.

Under the visible-light irradiation (λ = 520 ± 15 nm), the electrons are excited from the valence band (VB) of CdS NWs as the core in 1D CdS@TiO_2 CSNs to the conduction band (CB) of CdS, thereby forming the electron−hole pairs. Simultaneously, the photogenerated holes from the core of CdS NWs are stuck by the TiO_2 shell while the photogenerated electrons can transfer to the TiO_2 shell, because of their intimate interfacial contact and matchable energy band position.[73,74] This results in both the enhanced lifetime of charge carriers and the easy access to photogenerated electrons instead of holes. Molecular oxygen in the reaction system can be activated by accepting the photogenerated electrons, for example, the formation of superoxide radicals ($O_2^{\bullet -}$), as evidenced by the ESR analysis in Figure S2 in the Supporting Information. The substrate alcohols adsorbed on the surface of 1D CdS@TiO_2 CSNs can be oxidized by activated oxygen to give the target products: the corresponding aldehydes.

4. CONCLUDING REMARKS

In summary, 1D CdS@TiO_2 core−shell nanocomposites (CSNs) are successfully synthesized via a simple two-step solvothermal method. A uniform layer of TiO_2 shell is coated onto the CdS core, thus forming the 1D CdS core@TiO_2 shell semiconductor nanocomposites. Compared to the original 1D CdS nanowires (NWs), the as-obtained 1D CdS@TiO_2 CSNs show much-enhanced photocatalytic activities for selective oxidation of alcohols into corresponding aldehydes under visible-light irradiation. The enhanced photocatalytic perform-

ance can be attributed to the longer lifetime of photogenerated electron–hole pairs from the 1D CdS@TiO_2 CSNs, compared to the original 1D CdS NWs. In addition, it is interesting to find that the TiO_2 shell can also block the photogenerated holes from the CdS core, which leads to the conclusion that the reaction mechanism of photocatalytic oxidation of alcohols over 1D CdS@TiO_2 CSNs is apparently different from that over 1D CdS NWs under visible-light irradiation. It is hoped that our work could not only offer useful information on the fabrication of various specific 1D core–shell semiconductor nanostructures, but also open a new doorway to the use of such 1D core–shell semiconductors as visible-light photocatalysts in the field of selective transformations.

■ ASSOCIATED CONTENT

Ⓢ Supporting Information

The recycled testing of photocatalytic activity of the 1D CdS@TiO_2 CSNs toward the selective oxidation of benzyl alcohol to benzaldehyde data under visible-light irradiation (λ = 520 ± 15 nm) for 4 h, electron spin resonance (ESR) data under visible-light irradiation (λ = 520 ± 15 nm), and the photoactivity performance for photocatalytic reduction of Cr(VI) data under visible-light irradiation (λ = 520 ± 15 nm). This information is available free of charge via the Internet at http://pubs.acs.org.

■ AUTHOR INFORMATION

Corresponding Author

*Tel./Fax: +86 591 83779326. E-mail: yjxu@fzu.edu.cn.

Notes

The authors declare no competing financial interest.

■ ACKNOWLEDGMENTS

The support by the National Natural Science Foundation of China (Nos. 20903022, 20903023, 21173045), the Award Program for Minjiang Scholar Professorship, the Natural Science Foundation of Fujian Province for Distinguished Young Investigator Grant (No. 2012J06003), Program for Changjiang Scholars and Innovative Research Team in Universities (No. PCSIRT0818), Program for Returned High-Level Overseas Chinese Scholars of Fujian province, and the Project Sponsored by the Scientific Research Foundation for the Returned Overseas Chinese Scholars, State Education Ministry, is gratefully acknowledged.

■ REFERENCES

(1) Hines, M. A.; Guyot-Sionnest, P. *J. Phys. Chem.* **1996**, *100*, 468–471.
(2) Zhou, H. S.; Sasahara, H.; Honma, I.; Komiyama, H.; Haus, J. W. *Chem. Mater.* **1994**, *6*, 1534–1541.
(3) Kortan, A. R.; Hull, R.; Opila, R. L.; Bawendi, M. G.; Steigerwald, M. L.; Carroll, P. J.; Brus, L. E. *J. Am. Chem. Soc.* **1990**, *112*, 1327–1332.
(4) Haesselbarth, A.; Eychmueller, A.; Eichberger, R.; Giersig, M.; Mews, A.; Weller, H. *J. Phys. Chem.* **1993**, *97*, 5333–5340.
(5) Zhang, N.; Liu, S.; Fu, X.; Xu, Y.-J. *J. Phys. Chem. C* **2011**, *115*, 9136–9145.
(6) Zhang, N.; Fu, X.; Xu, Y.-J. *J. Mater. Chem.* **2011**, *21*, 8152–8158.
(7) Zhang, N.; Liu, S.; Fu, X.; Xu, Y.-J. *J. Mater. Chem.* **2012**, *22*, 5042–5052.
(8) Mandal, S.; Mandale, A. B.; Sastry, M. *J. Mater. Chem.* **2004**, *14*, 2868–2871.
(9) Cao, Y.; Jin, R.; Mirkin, C. A. *J. Am. Chem. Soc.* **2001**, *123*, 7961–7962.
(10) Sun, X.; Liu, J.; Li, Y. *Chem. Mater.* **2006**, *18*, 3486–3494.
(11) Caruso, F. *Adv. Mater.* **2001**, *13*, 11–22.
(12) Schärtl, W. *Adv. Mater.* **2000**, *12*, 1899–1908.
(13) Lei, Y.; Chim, W.-K. *J. Am. Chem. Soc.* **2005**, *127*, 1487–1492.
(14) Peng, X.; Schlamp, M. C.; Kadavanich, A. V.; Alivisatos, A. P. *J. Am. Chem. Soc.* **1997**, *119*, 7019–7029.
(15) Spanhel, L.; Haase, M.; Weller, H.; Henglein, A. *J. Am. Chem. Soc.* **1987**, *109*, 5649–5655.
(16) Kim, M.; Sohn, K.; Na, H. B.; Hyeon, T. *Nano Lett.* **2002**, *2*, 1383–1387.
(17) Lu, Y.; Yin, Y.; Li, Z.-Y.; Xia, Y. *Nano Lett.* **2002**, *2*, 785–788.
(18) Oldenburg, S. J.; Averitt, R. D.; Westcott, S. L.; Halas, N. J. *Chem. Phys. Lett.* **1998**, *288*, 243–247.
(19) Zhang, N.; Liu, S.; Xu, Y.-J. *Nanoscale* **2012**, *4*, 2227–2238.
(20) Zhang, N.; Liu, S.; Fu, X.; Xu, Y.-J. *J. Phys. Chem. C* **2011**, *115*, 22901–22909.
(21) Chang, W. K.; Koteswara Rao, K.; Kuo, H. C.; Cai, J. F.; Wong, M. S. *Appl. Catal., A* **2007**, *321*, 1–6.
(22) Lim, S. H.; Phonthammachai, N.; Pramana, S. S.; White, T. J. *Langmuir* **2008**, *24*, 6226–6231.
(23) Meng, H. L.; Cui, C.; Shen, H. L.; Liang, D. Y.; Xue, Y. Z.; Li, P. G.; Tang, W. H. *J. Alloys Compd.* **2012**, *527*, 30–35.
(24) Wang, L.; Wei, H.; Fan, Y.; Liu, X.; Zhan, J. *Nanoscale Res. Lett.* **2009**, *4*, 558–564.
(25) Banerjee, S.; Mohapatra, S. K.; Das, P. P.; Misra, M. *Chem. Mater.* **2008**, *20*, 6784–6791.
(26) Zhang, P.; Shao, C.; Zhang, Z.; Zhang, M.; Mu, J.; Guo, Z.; Liu, Y. *Nanoscale* **2011**, *3*, 2943–2949.
(27) Tachikawa, T.; Majima, T. *J. Am. Chem. Soc.* **2009**, *131*, 8485–8495.
(28) Tang, Z.-R.; Li, F.; Zhang, Y.; Fu, X.; Xu, Y.-J. *J. Phys. Chem. C* **2011**, *115*, 7880–7886.
(29) Xiao, F. *J. Phys. Chem. C* **2012**, *116*, 16487–16498.
(30) Tang, Z.-R.; Zhang, Y.; Xu, Y.-J. *ACS Appl. Mater. Interfaces* **2012**, *4*, 1512–1520.
(31) Xie, Y.; Ali, G.; Yoo, S. H.; Cho, S. O. *ACS Appl. Mater. Interfaces* **2010**, *2*, 2910–2914.
(32) Wang, X.; Li, S.; Yu, H.; Yu, J. *J. Mol. Catal. A: Chem.* **2011**, *334*, 52–59.
(33) Lee, W. J.; Lee, J. M.; Kochuveedu, S. T.; Han, T. H.; Jeong, H. Y.; Park, M.; Yun, J. M.; Kwon, J.; No, K.; Kim, D. H.; Kim, S. O. *ACS Nano* **2011**, *6*, 935–943.
(34) Fox, M. A.; Dulay, M. T. *Chem. Rev.* **1993**, *93*, 341–357.
(35) Maldotti, A.; Molinari, A.; Amadelli, R. *Chem. Rev.* **2002**, *102*, 3811–3836.
(36) Palmisano, G.; Augugliaro, V.; Pagliaro, M.; Palmisano, L. *Chem. Commun.* **2007**, 3425–3437.
(37) Zhang, Y.; Tang, Z.-R.; Fu, X.; Xu, Y.-J. *ACS Nano* **2011**, *5*, 7426–7435.
(38) Palmisano, G.; Garcia-Lopez, E.; Marci, G.; Loddo, V.; Yurdakal, S.; Augugliaro, V.; Palmisano, L. *Chem. Commun.* **2010**, *46*, 7074–7089.
(39) Zhang, M.; Wang, Q.; Chen, C.; Zang, L.; Ma, W.; Zhao, J. *Angew. Chem., Int. Ed.* **2009**, *48*, 6081–6084.
(40) Zhang, Y.; Zhang, N.; Tang, Z.-R.; Xu, Y.-J. *Phys. Chem. Chem. Phys.* **2012**, *14*, 9167–9175.
(41) Higashimoto, S.; Kitao, N.; Yoshida, N.; Sakura, T.; Azuma, M.; Ohue, H.; Sakata, Y. *J. Catal.* **2009**, *266*, 279–285.
(42) Augugliaro, V.; Caronna, T.; Loddo, V.; Marcì, G.; Palmisano, G.; Palmisano, L.; Yurdakal, S. *Chem.—Eur. J.* **2008**, *14*, 4640–4646.
(43) Zhang, N.; Zhang, Y.; Xu, Y.-J. *Nanoscale* **2012**, *4*, 5792–5813.
(44) Yurdakal, S.; Palmisano, G.; Loddo, V.; Augugliaro, V.; Palmisano, L. *J. Am. Chem. Soc.* **2008**, *130*, 1568–1569.
(45) Pillai, U. R.; Sahle-Demessie, E. *J. Catal.* **2002**, *211*, 434–444.
(46) Kominami, H.; Sugahara, H.; Hashimoto, K. *Catal. Commun.* **2010**, *11*, 426–429.
(47) Yurdakal, S.; Palmisano, G.; Loddo, V.; Alagoz, O.; Augugliaro, V.; Palmisano, L. *Green Chem.* **2009**, *11*, 510–516.
(48) Yang, X.; Wang, X.; Liang, C.; Su, W.; Wang, C.; Feng, Z.; Li, C.; Qiu, J. *Catal. Commun.* **2008**, *9*, 2278–2281.

(49) Palmisano, G.; Addamo, M.; Augugliaro, V.; Caronna, T.; Di Paola, A.; López, E. G.; Loddo, V.; Marcì, G.; Palmisano, L.; Schiavello, M. *Catal. Today* **2007**, *122*, 118−127.
(50) Palmisano, G.; Addamo, M.; Augugliaro, V.; Caronna, T.; Garcia-Lopez, E.; Loddo, V.; Palmisano, L. *Chem. Commun.* **2006**, 1012−1014.
(51) Chen, Y.; Wang, L.; Lu, G.; Yao, X.; Guo, L. *J. Mater. Chem.* **2011**, *21*, 5134−5141.
(52) Sang, L.; Tan, H.; Zhang, X.; Wu, Y.; Ma, C.; Burda, C. *J. Phys. Chem. C* **2012**, *116*, 18633−18640.
(53) Lin, C. J.; Yu, Y. H.; Liou, Y. H. *Appl. Catal., B* **2009**, *93*, 119−125.
(54) Wang, C.; Sun, L.; Xie, K.; Lin, C. *Sci. China, Ser. B* **2009**, *52*, 2148−2155.
(55) Zhu, H.; Yang, B.; Xu, J.; Fu, Z.; Wen, M.; Guo, T.; Fu, S.; Zuo, J.; Zhang, S. *Appl. Catal., B* **2009**, *90*, 463−469.
(56) Radovanovic, P. V.; Barrelet, C. J.; Gradečak, S.; Qian, F.; Lieber, C. M. *Nano Lett.* **2005**, *5*, 1407−1411.
(57) Routkevitch, D.; Bigioni, T.; Moskovits, M.; Xu, J. M. *J. Phys. Chem.* **1996**, *100*, 14037−14047.
(58) Zhang, D.; Wang, Y. *Mater. Sci. Eng., B* **2006**, *134*, 9−19.
(59) Wang, L.; Wei, H.; Fan, Y.; Gu, X.; Zhan, J. *J. Phys. Chem. C* **2009**, *113*, 14119−14125.
(60) Zhang, Y.; Zhang, N.; Tang, Z.-R.; Xu, Y.-J. *Chem. Sci.* **2012**, *3*, 2812−2822.
(61) Carp, O.; Huisman, C. L.; Reller, A. *Prog. Solid State Chem.* **2004**, *32*, 33−177.
(62) Zhang, Y.; Zhang, N.; Tang, Z.-R.; Xu, Y.-J. *ACS Nano* **2012**, DOI: 10.1021/nn304154s.
(63) Yao, W.; Ye, J. *J. Phys. Chem. B* **2006**, *110*, 11188−11195.
(64) Pillai, Z. S.; Kamat, P. V. *J. Phys. Chem. B* **2003**, *108*, 945−951.
(65) Chen, C.; Wang, Q.; Lei, P.; Song, W.; Ma, W.; Zhao, J. *Environ. Sci. Technol.* **2006**, *40*, 3965−3970.
(66) Carbone, L.; Nobile, C.; De Giorgi, M.; Sala, F. D.; Morello, G.; Pompa, P.; Hytch, M.; Snoeck, E.; Fiore, A.; Franchini, I. R.; Nadasan, M.; Silvestre, A. F.; Chiodo, L.; Kudera, S.; Cingolani, R.; Krahne, R.; Manna, L. *Nano Lett.* **2007**, *7*, 2942−2950.
(67) Chiu, W.; Khiew, P.; Cloke, M.; Isa, D.; Lim, H.; Tan, T.; Huang, N.; Radiman, S.; Abd-Shukor, R.; Hamid, M. A. A.; Chia, C. *J. Phys. Chem. C* **2010**, *114*, 8212−8218.
(68) Fiore, A.; Mastria, R.; Lupo, M. G.; Lanzani, G.; Giannini, C.; Carlino, E.; Morello, G.; De Giorgi, M.; Li, Y.; Cingolani, R.; Manna, L. *J. Am. Chem. Soc.* **2009**, *131*, 2274−2282.
(69) Xu, D.; Liu, Z.; Liang, J.; Qian, Y. *J. Phys. Chem. B* **2005**, *109*, 14344−14349.
(70) Xi, Y.; Zhou, J.; Guo, H.; Cai, C.; Lin, Z. *Chem. Phys. Lett.* **2005**, *412*, 60−64.
(71) Li, Y.; Liao, H.; Ding, Y.; Fan, Y.; Zhang, Y.; Qian, Y. *Inorg. Chem.* **1999**, *38*, 1382−1387.
(72) Zhang, N.; Zhang, Y.; Pan, X.; Fu, X.; Liu, S.; Xu, Y.-J. *J. Phys. Chem. C* **2011**, *115*, 23501−23511.
(73) Zhang, N.; Zhang, Y.; Pan, X.; Yang, M.-Q.; Xu, Y.-J. *J. Phys. Chem. C* **2012**, *116*, 18023−18031.
(74) Das, K.; De, S. K. *J. Phys. Chem. C* **2009**, *113*, 3494−3501.